

# KERNFORSCHUNGSZENTRUM KARLSRUHE

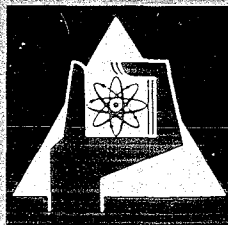
Juni 1970

KFK 1230  
IAEA-CN-26/11a

Institut für Angewandte Kernphysik

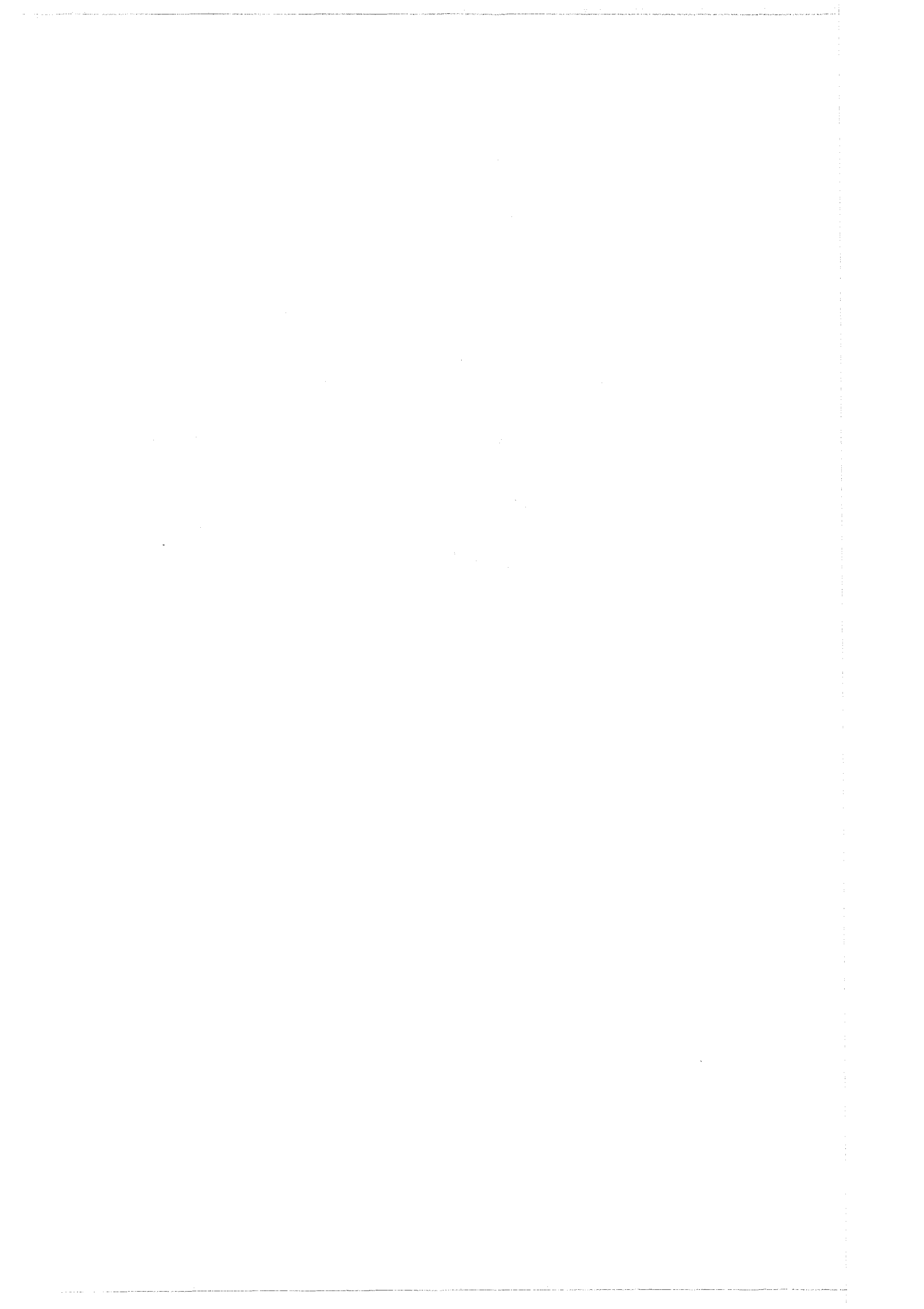
Total Cross Sections of  $^{45}\text{Sc}$ ,  $^{47}\text{Ti}$ ,  $^{49}\text{Ti}$ ,  $^{53}\text{Cr}$ , and  $^{61}\text{Ni}$   
in the keV Region

M. Cho, F.H. Fröhner, M. Kazerouni, K.-N. Müller, G. Rohr



GESELLSCHAFT FÜR KERNFORSCHUNG M.B.H.

KARLSRUHE



KERNFORSCHUNGSZENTRUM KARLSRUHE

Juni 1970

KFK 1230  
IAEA-CN-26/11a

Institut für Angewandte Kernphysik

Total Cross Sections of  $^{45}\text{Sc}$ ,  $^{47}\text{Ti}$ ,  $^{49}\text{Ti}$ ,  $^{53}\text{Cr}$ , and  $^{61}\text{Ni}$   
in the keV Region \*)

M. Cho, F.H. Fröhner, M. Kazerouni, K.-N. Müller, and G. Rohr

\*) Paper presented at the Second International Conference on Nuclear Data for Reactors, Helsinki 1970



## ZUSAMMENFASSUNG

Es wurden totale Wirkungsquerschnitte für separierte Isotope mit dem Flugzeitspektrometer am Karlsruher 3 MeV Van-de-Graaff-Generator gemessen. Die Neutronenenergien lagen zwischen 10 und 250 keV, die Zeitauflösung zwischen 0.2 und 0.5 nsec/m.

Zur Analyse der gemessenen Wirkungsquerschnitte wurden diese durch eine R-Matrix-Multiniveauformel beschrieben. So konnten Neutronenbreiten und Spins für bis zu 50 Resonanzen pro Isotop bestimmt werden. Mittlere Niveaubreiten, Niveaudichten und Stärkefunktionswerte wurden ermittelt, und es wurden die Spinabhängigkeit der Stärkefunktion und die Verteilung von Niveaubreiten und -abständen untersucht.



Total Cross Sections of  $^{45}\text{Sc}$ ,  $^{47}\text{Ti}$ ,  $^{49}\text{Ti}$ ,  $^{53}\text{Cr}$ , and  $^{61}\text{Ni}$   
in the keV region

M. CHO, F.H. FRÖHNER, M. KAZEROUNI, K.-N. MÜLLER, and G. ROHR

Kernforschungszentrum Karlsruhe  
Karlsruhe, Federal Republic of Germany

## ABSTRACT

Neutron total cross sections of separated isotopes were measured with the time-of-flight spectrometer at the 3 MeV Karlsruhe Van de Graaff Accelerator. The neutron energy ranged from 10 to 250 keV. The energy resolution was between 0.2 and 0.5 nsec/m.

The measured cross sections were shape-analyzed in terms of an R-matrix multilevel formula. Thus neutron widths and spins for up to 50 resonances per isotope could be determined. Average neutron widths, level densities and strength functions were derived. The spin dependence of strength functions and the distribution of widths and spacings were investigated.

## 1. INTRODUCTION

High resolution measurements of neutron total cross sections in the keV-region are of interest, both for the construction of fast breeders, and for the investigation of physical questions. The keV-spectrometer, installed at the pulsed 3 MeV Karlsruhe Van de Graaff generator, is characterized by high resolution and by the need for only gram-amounts of sample material. This allows the measurement of separated isotopes. The nuclei studied in Karlsruhe are selected according to these facts from the mass region between  $A = 40$  and  $A = 70$ . For this region and for neutron energies  $E_n = 10$  to 250 keV, most of the cross section is due to elastic scattering, because the

capture widths are small compared to the neutron widths and in most cases further reactions are not possible.

The analysis of the measured cross section requires the use of a multi-level formula, which can describe the level-level interference effects due to overlapping resonances of the same spin state. The parametrization of the cross section yields resonance parameters, which allow investigations of level densities, strength functions, and distributions of level widths and spacings.

## 2. EXPERIMENTAL METHOD AND ANALYZING TECHNIQUES

The total cross section was measured in a transmission experiment by the time-of-flight method. Neutrons were generated in a thick lithium target by the (p,n) reaction. The flight time was measured with a digital time coder. For energies up to about 60 keV a boron slab detector was used and a proton recoil detector at higher energies. The resolution was between 0.2 and 0.5 nsec/m for flight paths of 6, 10, and 22 meters. To eliminate fluctuations of the neutron yield, an automatic sample changer, controlled by a beam current integrator, was used. More detailed descriptions of the experimental set-up are already published [1,2].

With the exception of Scandium all sample materials were provided by the EANDC-Pool. Scandium was used in the form of metal plates, the titanium isotopes as  $TiO_2$  powder enriched to 79.5 % (16.5 %  $^{48}Ti$ ) in the case of  $^{47}Ti$  and to 76.1 % (18.5 %  $^{48}Ti$ ) in the case of  $^{49}Ti$ .  $^{53}Cr$  was available in the form of 5.8 g  $Cr_2O_3$  powder enriched to 95.2 % (2.7 %  $^{52}Cr$ ) and  $^{61}Ni$  as metal powder enriched to 91.78 % (5.2 %  $^{60}Ni$ ). The material was filled into thin-walled aluminum containers. In the measurements without sample, equivalent empty containers were used. Different sample thicknesses, depending on the energy range and the cross section structure, were chosen in order to get optimal statistical error and inscattering conditions. The influence of the oxygen content of the samples is easily corrected for, because its cross section, 3.5 barns, is constant up to 300 keV.

For analysis of the cross section, an R-matrix multi-level formula [3] was used. Because of the minimum of the p-wave strength function in the mass region under consideration and because of the low penetration factors for higher partial waves in the keV region, all resonances of analyzable width were assumed to be due to s-wave neutrons. The fits to the  $^{49}Ti$  and  $^{53}Cr$  data were achieved by trial and error. For the other isotopes a least squares fit program was written. The influence of the resonances outside the analyzed region [4] was taken into account using a scattering phase of the form

$$\varphi_{oJ} = k \cdot a (1 - R_{oJ}^{\infty})$$

with  $R_{oJ}^{\infty} = A_J + B_J (E - E_M) + C_J (E - E_M)^2$

Here  $k$  is the wave number,  $a$  the nuclear radius and  $E_M$  the middle of the energy interval analyzed. The coefficients  $A_J$ ,  $B_J$ , and  $C_J$  were chosen to give the best fit in the valleys between resonance peaks.

### 3. RESULTS

The cross sections obtained are presented in the figures 1 to 5. The points give the experimental values and the curves give the fits achieved. The resonance parameters (resonance energy  $E_\lambda$ , width  $\Gamma_\lambda$ , and spin state  $J$ ) yielding these fits are collected in Tables I to VI. Table VII contains the parameters describing the influence of the resonances outside of the analyzed region.

The Scandium data reveal a very high level density. Because of the many resonances analyzed, an investigation of the distribution of widths and spacings was possible. Fig. 6 shows the experimental distributions in the usual integrated form. The theoretical curves - Porter-Thomas distributions of the widths and Wigner distributions of the spacings - are plotted as smooth curves. The agreement between experimental and theoretical distributions is obvious.

Because of the relatively high  $^{48}\text{Ti}$  content of the two Titanium samples a separate multi-level fit to the Columbia measurements [5] of natural Titanium (73.9 %  $^{48}\text{Ti}$ ) was carried out. The curve in fig. 2a shows the fit obtained with the parameters of the first 4 resonances listed in Table III. The points are typical Columbia values. The cross section contribution of these four resonances is easily visible in the data obtained for both Titanium samples. The parameters of the other resonances listed in Table III were estimated from the Columbia data but they could not be uniquely identified with our measured resonance structures.

An important point in the parametrization of the  $^{53}\text{Cr}$  cross section is the existence of a big spin-one resonance at 135 keV and a superposition of two resonances of different spin states at 124 keV. This interpretation is based e.g. on the slow rise and steep decline of the 124 keV structure. Such a shape contrary to the normally steep rise and slow decline of an isolated resonance is typical for an interference with a big higher energy resonance of the same spin. The influence of the big spin-one resonance on the spin dependence of the strength function is decisive. The strength function, evaluated for the energy range up to 120 keV, does not show a spin dependence. Because of the 135 keV resonance the strength function for spin 1 calculated for the whole range up to 250 keV is twice that for spin two.

The influence of the  $^{52}\text{Cr}$  content of the Chromium samples was taken into account using the Duke [3] resonance parameters. For Nickel the  $^{60}\text{Ni}$  resonances at 12.5 keV ( $\Gamma_\lambda = 2.6$  keV) and 28.7 keV ( $\Gamma_\lambda = 1.11$  keV) [3,5] were considered. The influence of the 12.5 keV resonance was clearly evident as a background structure lifting up the interference

valleys of the two spin 2 resonances at 12.7 and 13.6 keV. For  $^{52}\text{Cr}$   $A = B = C = 0$  was chosen, and  $A = -0.15$ ,  $B = C = 0$  for  $^{60}\text{Ni}$  [3].

The statistical parameters obtained from the analyzed resonances are listed in Table VIII. The average level distance  $\bar{D}$ , the average reduced width  $\bar{\Gamma}_n^0$ , the s-wave neutron strength function  $S$ , and the number of levels are listed in an (a) and a (b) version. Version (a) gives the values obtained directly from the analyzed resonances. Due to the energy dependent detection and analyzing limit for resonances, levels are missed. In the case (b) a correction for these "missed levels" [6] was carried out. It is based on the assumption of the validity of the Porter-Thomas distribution for the level widths. Though many levels are missed in some cases, their contribution to the strength function is small in general. A more pronounced difference between (a) and (b) strength function values (e.g.  $^{45}\text{Sc}$ ) is due to low average level widths relative to the detection threshold.

For some of the measured isotopes a spin dependence of the strength function was found, for others not. At the moment no general description or explanation for the observed spin dependence is available. Recent calculations of strength functions in the 3s-resonance region [7], carried out for nuclei with and without spin, yielded a good description of the fluctuations of experimental strength functions around the optical model values. This agreement between calculations and experiment can be interpreted as an indication for a spin independence of the strength function [8]. A spin dependence would be caused by shell effects producing a deviation from the average spin dependence of the doorway-state density. The existing experimental data in general do not show a systematic tendency, if one compares spin-up and spin-down strength functions [9].

With the exception of  $^{45}\text{Sc}$  all nuclei had already been measured by the Oak Ridge Group [10] in the energy range of about 3 to 50 keV. The advantage of the present measurement is a resolution improvement of a factor ten and the extension of the energy range. Moreover a thorough analysis of the data was carried out. The use of a multi-level formula allows a description of most of the complicated cross section structures occurring. A fit of the typical interference shapes yields a determination of spins even in the case of not completely resolved resonances.

REFERENCES

- [1] ROHR, G., thesis, Karlsruhe University, 1967
- [2] ROHR, G., MÜLLER, K.-N., Zeitschr. Phys. 227 (1969) 1
- [3] BOWMAN, C.D., BILPUCH, E.G., NEWSON, H.W., Ann. Phys. 17 (1962) 319
- [4] FIRK, F.W.K., LYNN, J.E., MOXON, M.C., Proc. Phys. Soc. 82 (1963) 477
- [5] GARG, J.G., RAINWATER, J., HAVENS Jr., W.W., FANDC(US) - 54 "L", CR-1860
- [6] FUKETA, T., HARVEY, J.A., Nucl. Instrum. Meth. 33 (1965) 107
- [7] MÜLLER, K.-N., ROHR, G., KFK-Report 1114, Karlsruhe 1969
- [8] MÜLLER, K.-N., ROHR, G., to be published
- [9] MALETSKI, KH., PIKELNER, L.B., SALAMATIN, I.M., SHARAPOV, E.I., JINR-P<sub>3</sub>-4484, Dubna 1969
- [10] GOOD, W.M., PAYA, D., WAGNER, R., TAMURA, T., Phys. Rev. 151 (1966) 912



Table I : Resonance parameters of  $^{45}\text{Sc}$

$E_\lambda^*)$	$\Gamma_\lambda^*)$	$(2g\Gamma)_\lambda^*)$	J	$E_\lambda^*)$	$\Gamma_\lambda^*)$	$(2g\Gamma)_\lambda^*)$	J
19.17	0.06	0.0675	4	65.94	1.04	1.17	4
20.80	0.06	0.0675	4	70.11	1.69	1.48	3
20.95	0.8	0.7	3	71.76	0.41	0.46	4
24.18	0.06	0.0525	3	73.18	0.35	0.307	3
24.48	0.06	0.0675	4	74.90	0.15	0.131	3
27.12	0.09	0.1012	4	77.15	0.25	0.28	4
28.12	0.11	0.09625	3	77.55	0.6	0.525	3
29.85	0.1	0.1125	4	77.85	0.15	0.168	4
32.40	0.57	0.4987	3	79.00	0.2	0.175	3
34.0	0.19	0.166	3	79.80	2.8	2.45	3
35.3	0.28	0.315	4	81.10	0.6	0.675	4
40.37	0.13	0.146	4	83.00	0.15	0.169	4
40.77	0.10	0.0875	3	85.60	0.85	0.956	4
41.15	0.11	0.124	4	86.00	0.65	0.569	3
43.35	0.17	0.19	4	88.60	0.55	0.481	3
46.15	0.48	0.42	3	90.20	0.12	0.135	4
47.60	0.18	0.1575	3	91.70	0.55	0.481	3
49.17	0.16	0.18	4	94.40	0.8	0.7	3
51.16	0.84	0.952	4	99.80	2.0	1.75	3
52.18	0.1	0.091	3	100.7	0.3	0.337	4
54.83	0.22	0.193	3	101.0	0.4	0.35	3
57.68	0.22	0.189	3	102.1	0.3	0.337	4
58.77	1.64	1.438	3	102.3	0.35	0.306	3
61.84	0.52	0.589	4	104.0	0.15	0.169	4
62.54	0.57	0.494	3	105.7	0.15	0.169	4

\*<sup>)</sup> keV

errors of energies ~ 0.3 %  
errors of widths ~ 10 %

Table II : Resonance parameters of  $^{47}\text{Ti}$

$E_\lambda^*)$	$\Gamma_\lambda^*)$	$(2g\Gamma)_\lambda^*)$	J	$E_\lambda^*)$	$\Gamma_\lambda^*)$	$(2g\Gamma)_\lambda^*)$	J
8.14	0.066	0.055	2	40.37	0.692	0.807	3
8.32	0.147	0.122	2	41.03	0.058	0.048	2
10.54	0.058	0.068	3	42.23	0.582	0.484	2
12.13	0.120	0.140	3	42.08	0.881	1.027	3
12.16	0.022	0.018	2	46.40	0.706	0.823	3
12.81	0.175	0.146	2	49.27	0.315	0.367	3
16.38	0.396	0.462	3	51.34	0.180	0.210	3
17.39	0.050	0.042	2	55.37	0.276	0.322	3
19.08	0.020	0.023	3	57.56	0.859	1.002	3
21.26	0.062	0.052	2	60.29	0.089	0.074	2
27.12	0.111	0.092	2	61.78	0.213	0.177	2
27.17	0.957	1.116	3	63.37	0.097	0.113	3
30.18	0.074	0.062	2	63.80	0.053	0.062	3
32.33	0.599	0.498	2	71.68	0.490	0.571	3
38.11	0.080	0.093	3	74.55	0.128	0.107	2

\*<sup>)</sup> keV

errors of energies ~ 0.3 %  
errors of widths ~ 10 %

Table III : Resonance parameters of  $^{48}\text{Ti}$

$E_\lambda$ *)	$\Gamma_\lambda$ *)	$(2g\Gamma)_\lambda$ *)	J	$E_\lambda$ *)	$\Gamma_\lambda$ *)	$(2g\Gamma)_\lambda$ *)	J
17.76	8.43	16.86	0.5	119.0	0.2	0.4	0.5
22.11	0.78	1.56	0.5	133.2	0.2	0.4	0.5
36.9	1.3	2.6	0.5	154.9	0.25	0.5	0.5
51.7	2.4	4.8	0.5	185.6	0.65	1.3	0.5
74.4	0.15	0.3	0.5	192.4	3.0	6.0	0.5
83.6	0.12	0.24	0.5				

\*) keV

Table IV : Resonance parameters of  $^{49}\text{Ti}$

$E_\lambda$ *)	$\Gamma_\lambda$ *)	$(2g\Gamma)_\lambda$ *)	J	$E_\lambda$ *)	$\Gamma_\lambda$ *)	$(2g\Gamma)_\lambda$ *)	J
18.76	$0.09 \pm 0.01$	0.10	4	151.2	$3.3 \pm 1.0$	2.9	3
21.54	$0.15 \pm 0.04$	0.13	3	152.2	$2.8 \pm 1.0$	3.1	4
22.77	$0.70 \pm 0.10$	0.61	3	170.5	$0.8 \pm 0.2$	0.9	4
27.14	$0.42 \pm 0.05$	0.47	4	172.3	$3.5 \pm 0.7$	3.9	4
31.9	$2.0 \pm 0.2$	2.3	4	176.2	$1.8 \pm 0.5$	2.0	4
38.4	$1.7 \pm 0.2$	1.9	4	184.7	$3.0 \pm 0.6$	2.6	3
56.1	$0.45 \pm 0.1$	0.5	4	185.8	$2.5 \pm 0.5$	2.8	4
59.4	$0.45 \pm 0.1$	0.39	3	187.7	$4.0 \pm 1.0$	3.5	3
66.75	$0.8 \pm 0.1$	0.7	3	197.0	$3.0 \pm 0.6$	3.4	4
76.6	$0.9 \pm 0.2$	1.0	4	208.5	$1.5 \pm 0.3$	1.3	3
96.6	$3.0 \pm 0.5$	2.6	3	216.0	$2.2 \pm 0.4$	2.5	4
106.4	$3.3 \pm 0.5$	2.9	3	224.5	$2.0 \pm 0.4$	1.8	3
138.8	$1.6 \pm 0.2$	1.8	4	239.0	$2.0 \pm 0.5$	2.3	4
145.7	$1.9 \pm 0.3$	1.7	3				

\*) keV

Table V : Resonance parameters of  $^{53}\text{Cr}$

$E_\lambda$ *)	$\Gamma_\lambda$ *)	$(2g\Gamma)_\lambda$ *)	J	$E_\lambda$ *)	$\Gamma_\lambda$ *)	$(2g\Gamma)_\lambda$ *)	J
19.53	$0.13 \pm 0.02$	0.16	2	135.0	$24.0 \pm 5.0$	18.0	1
25.64	$0.22 \pm 0.03$	0.28	2	145.9	$0.6 \pm 0.1$	0.8	2
26.95	$0.70 \pm 0.10$	0.53	1	157.8	$0.9 \pm 0.1$	1.1	2
29.23	$0.33 \pm 0.03$	0.41	2	159.0	$2.0 \pm 0.3$	2.5	2
65.7	$4.5 \pm 0.07$	5.6	2	172.7	$1.2 \pm 0.2$	1.5	2
73.1	$1.05 \pm 0.25$	0.8	1	175.7	$4.0 \pm 0.8$	3.0	1
74.06	$1.2 \pm 0.2$	1.5	2	183.0	$3.5 \pm 0.7$	2.6	1
87.2	$7.8 \pm 1.0$	5.9	1	186.0	$0.5 \pm 0.2$	0.6	2
94.5	$0.6 \pm 0.1$	0.75	2	195.7	$0.6 \pm 0.1$	0.8	2
99.7	$0.4 \pm 0.1$	0.3	1	201.7	$0.55 \pm 0.1$	0.7	2
107.4	$1.5 \pm 0.15$	1.9	2	221.6	$4.2 \pm 0.8$	5.2	2
123.6	$4.0 \pm 1.0$	3.0	1	227.5	$0.3 \pm 0.1$	0.4	2
124.5	$0.5 \pm 0.2$	0.6	2	239.0	$3.0 \pm 0.6$	3.8	2
127.6	$0.4 \pm 0.2$	0.5	2	244.5	$4.0 \pm 1.0$	3.0	1
129.5	$0.2 \pm 0.1$	0.3	2	246.0	$0.5 \pm 0.3$	0.6	2

\*) keV

Table VI : Resonance parameters of  $^{61}\text{Ni}$

$E_{\lambda}^{\dagger}$	$\Gamma_{\lambda}^{\dagger}$	$(2g\Gamma)_{\lambda}^{\dagger}$	J	$E_{\lambda}^{\ddagger}$	$\Gamma_{\lambda}^{\ddagger}$	$(2g\Gamma)_{\lambda}^{\ddagger}$	J
7.15	0.074	0.056	1	33.68	0.058	0.044	1
7.55	0.177	0.221	2	37.13	0.133	0.166	2
8.74	0.006	0.008	2	41.34	0.176	0.132	1
12.64	0.075	0.094	2	43.25	0.010	0.013	2
13.63	0.061	0.076	2	43.61	0.030	0.038	2
14.02	0.017	0.013	1	45.49	0.066	0.050	1
16.70	0.817	0.613	1	46.16	0.054	0.041	1
17.86	0.177	0.133	1	50.51	0.133	0.100	1
18.87	0.069	0.086	2	53.30	0.141	0.176	2
24.62	0.129	0.097	1	54.81	0.189	0.142	1
28.21	0.003	0.004	2	56.49	0.119	0.149	2
29.11	0.409	0.307	1	58.16	0.178	0.134	1
30.64	0.013	0.016	2	64.07	0.535	0.669	2
31.13	0.788	0.591	1	65.87	1.430	1.788	2
31.83	0.008	0.010	2	68.77	1.100	1.375	2
32.70	0.220	0.275	2				

$\dagger$  keV

errors of energies  $\sim 0.3 \%$   
errors of widths  $\sim 10 \%$

Table VII : Parameters for  $R_{0J}^{\infty}$

Target nucleus	$E_H$	$A_J$	B	$C(E < E_H)$	$C(E > E_H)$
$^{45}\text{Sc}$	60 keV	0.2	0.01	$-1.0 \cdot 10^{-6}$	$+1.0 \cdot 10^{-6}$
$^{47}\text{Ti}$	-	$J=2 - 0.63$ $J=3 + 0.14$	0	0	0
$^{48}\text{Ti}$	-	0.33	0	0	0
$^{49}\text{Ti}$	130 keV	$2.6 \cdot 10^{-1}$	$1.9 \cdot 10^{-3}$	$-5.5 \cdot 10^{-6}$	$+5.5 \cdot 10^{-6}$
$^{53}\text{Cr}$	160 keV	$2.8 \cdot 10^{-3}$	$2.33 \cdot 10^{-3}$	$-2.22 \cdot 10^{-5}$	$+2.22 \cdot 10^{-5}$
$^{61}\text{Ni}$	-	$J=1 + 0.12$ $J=2 - 0.23$	0	0	0

Table VIII : Averaged values

Target nucleus	spin state	energy range (keV)	$\bar{D}$ (keV)		$\bar{\Gamma}_n^o$ (eV)		$S \cdot 10^4$		number of levels	
			a	b	a	b	a	b	a	b
$^{45}\text{Sc}$	$J = 3$	19 - 107	3.13	2.15	2.37	1.66	7.6	7.7	26	38
	$J = 4$		3.76	1.98	1.18	0.67	3.2	3.4	24	46
	independent		1.77	1.10	1.75	1.13	5.0	5.1	50	80
$^{47}\text{Ti}$	$J = 2$	8 - 76	5.11	3.04	1.0	0.6	2.0	2.1	14	24
	$J = 3$		4.08	2.95	2.0	1.4	4.8	4.9	16	22
	independent		2.29	1.59	1.6	1.1	3.5	3.6	30	43
$^{49}\text{Ti}$	$J = 3$	17 - 250	18.45	13.41	5.6	4.1	3.1	3.1	12	17
	$J = 4$		15.73	11.06	5.1	3.6	3.2	3.3	15	21
	independent		8.47	6.04	5.3	3.9	3.2	3.2	27	38
$^{53}\text{Cr}$	$J = 1$	18 - 250	27.19	22.70	15.4	12.9	5.7	5.7	9	11
	$J = 2$		11.32	6.91	3.2	2.1	2.9	3.0	21	38
	independent		7.81	5.73	6.3	4.7	4.0	4.1	30	41
$^{61}\text{Ni}$	$J = 1$	7 - 69	3.92	2.79	1.4	1.0	3.7	3.7	14	20
	$J = 2$		3.83	2.44	1.1	0.7	2.9	3.0	17	27
	independent		2.05	1.36	1.3	0.9	3.1	3.2	31	47

a only number of analyzed levels used  
b "missed levels" included



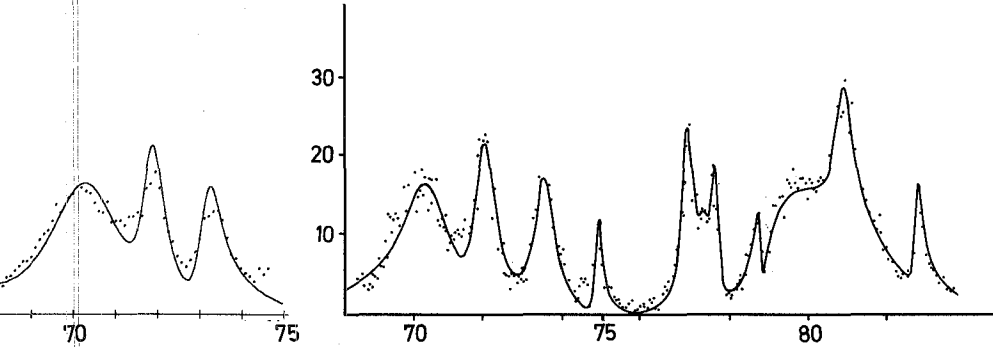
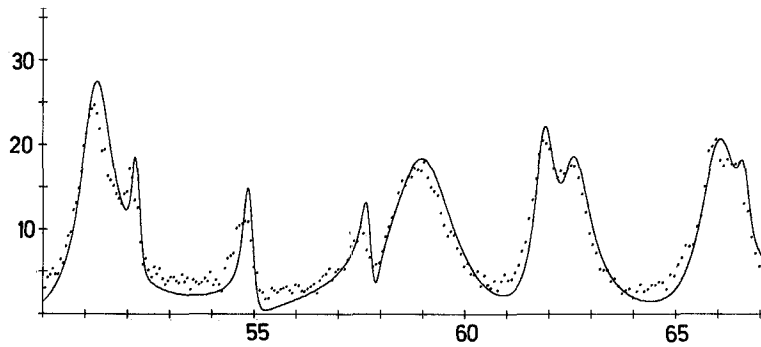
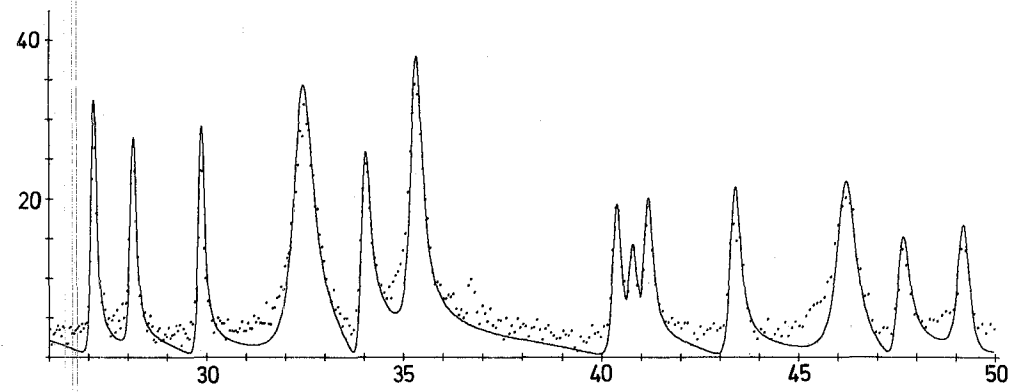
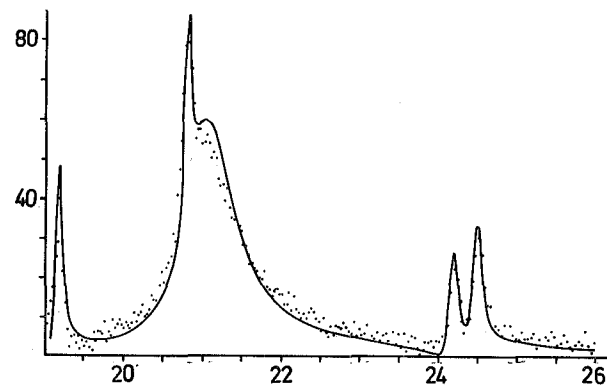
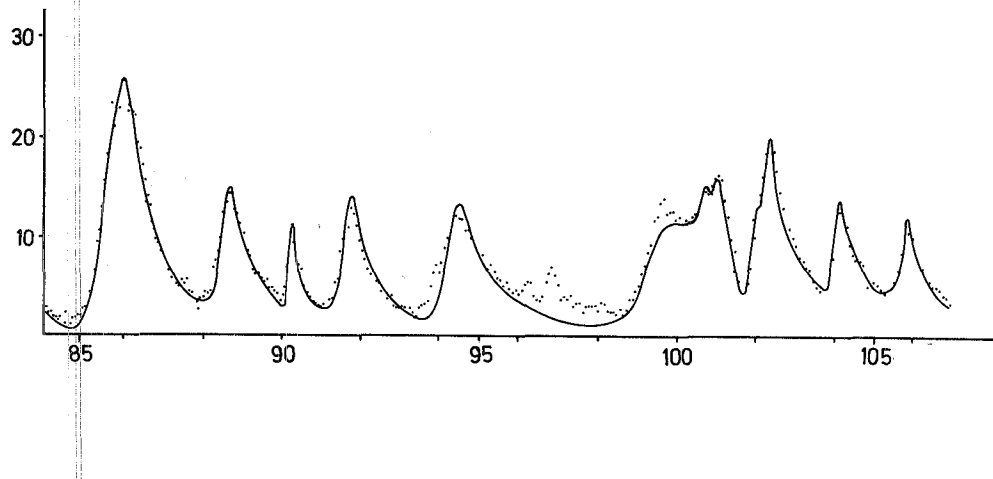


Fig.1. Total neutron cross section for  $^{45}\text{Sc}$   
X-axis:  $\sigma_{\text{tot}}$  (barn)  
Y-axis:  $E_n$  (keV)



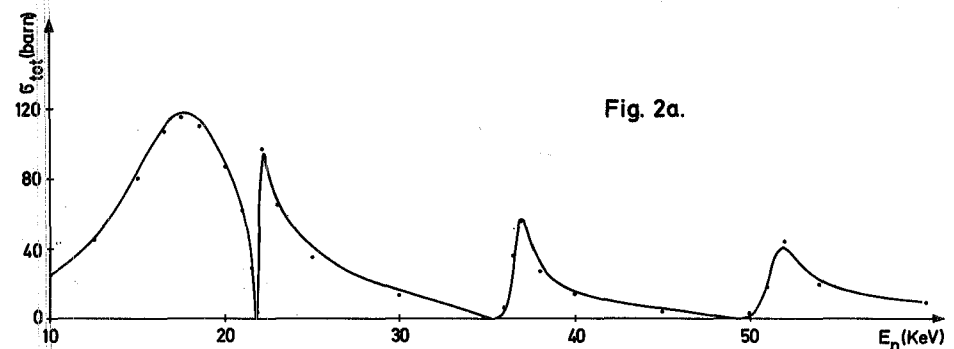
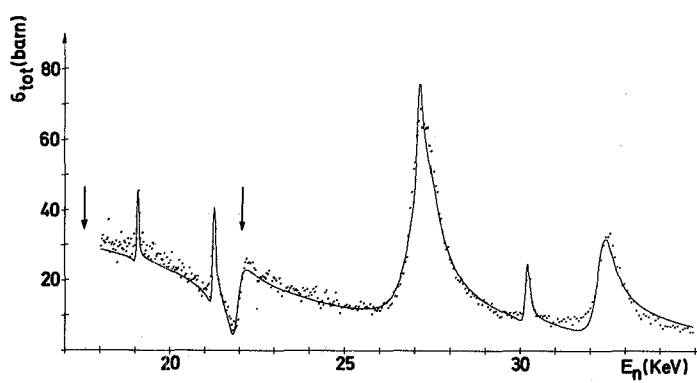
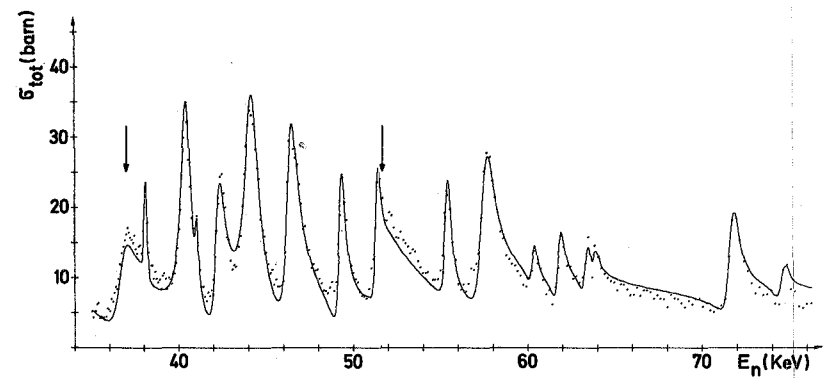
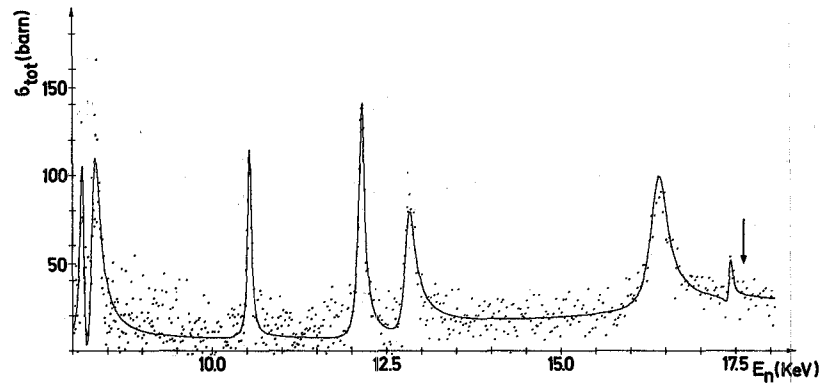


Fig. 2. Total neutron cross section curve for  $^{47}\text{Ti}$

$0.795 \sigma(\text{Ti 47}) + 0.165 \sigma(\text{Ti 48})$ , Arrows indicate  $^{48}\text{Ti}$  resonances,

Fig. 2a. Total neutron cross section curve for  $^{48}\text{Ti}$ ,  $0.739 \sigma(\text{Ti 48})$

Fig. 2a.

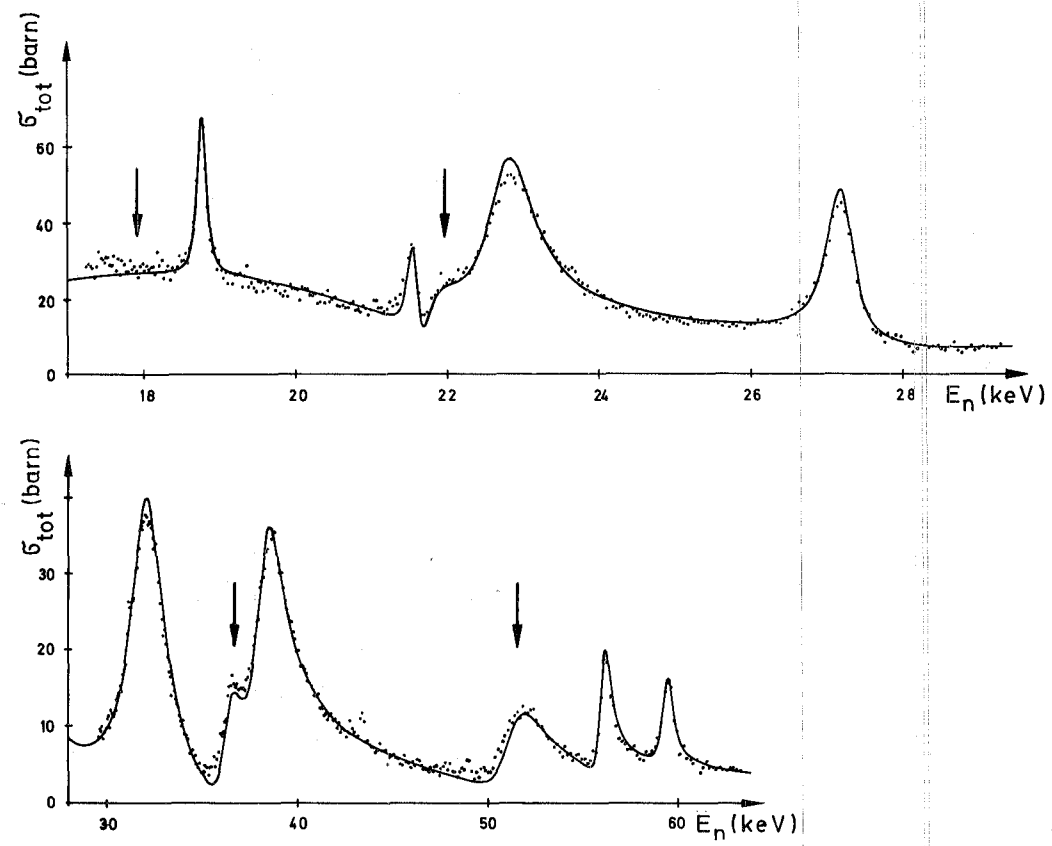
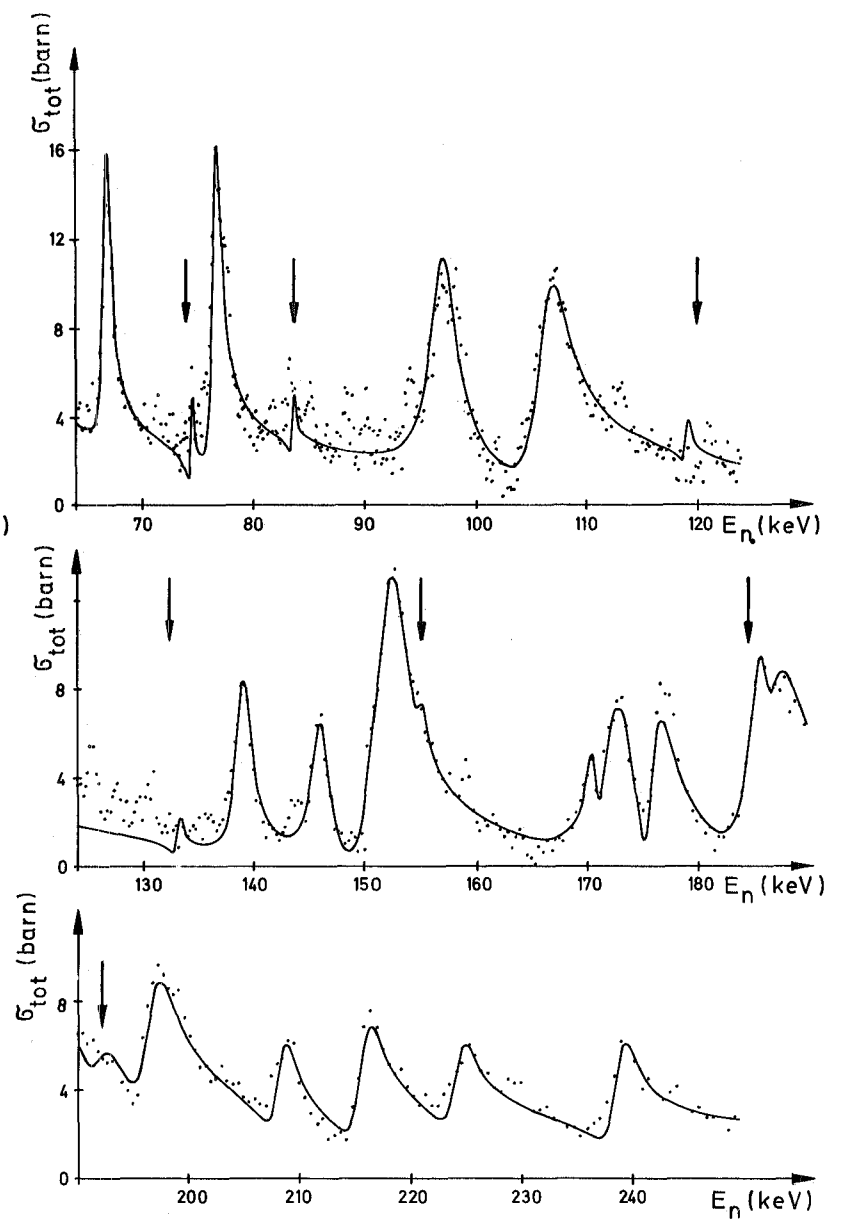


Fig.3. Total neutron cross section curve for  $^{49}\text{Ti}$   
 $0.761 \sigma(\text{Ti } 49) + 0.185 \sigma(\text{Ti } 48)$ , Arrows indicate  $^{48}\text{Ti}$  resonances



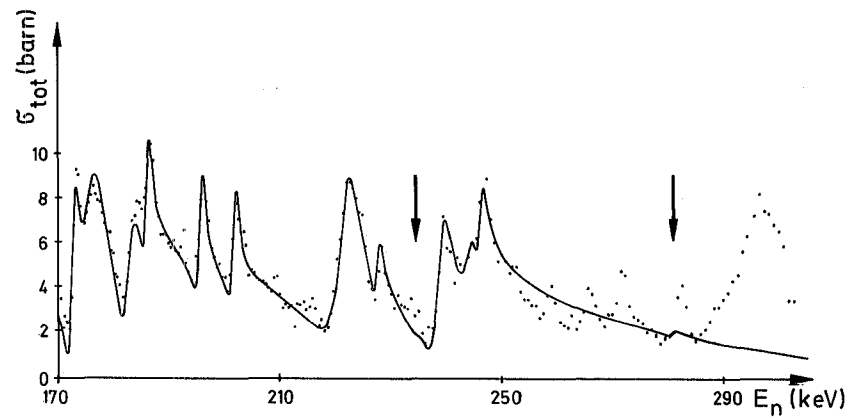
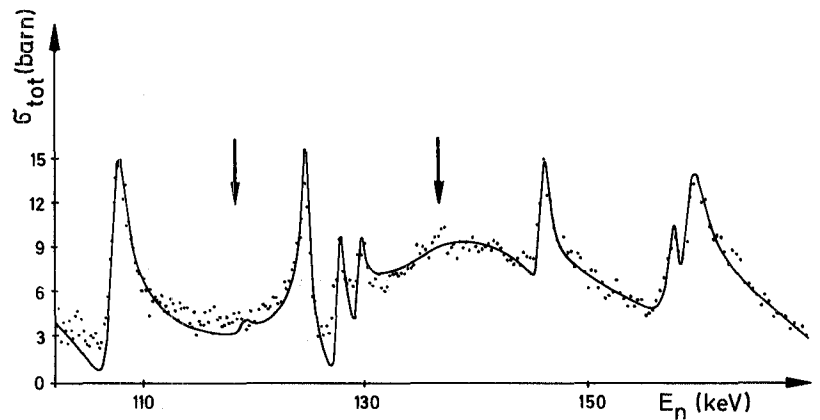
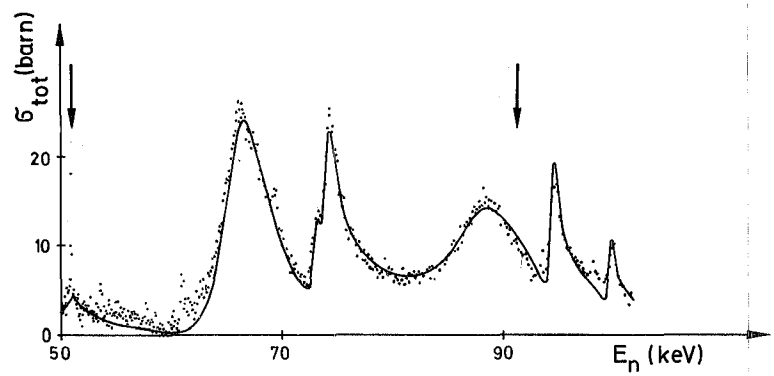
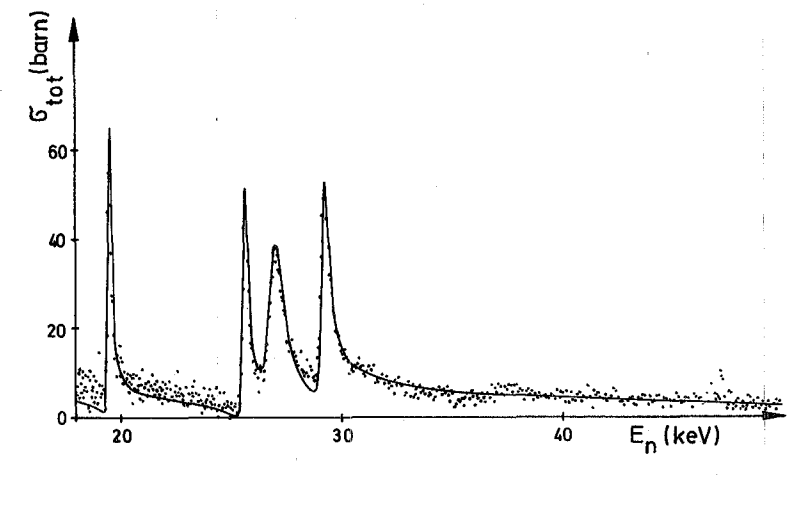


Fig.4. Total neutron cross section curve for  $^{53}\text{Cr}$   
 $0.952 \sigma(\text{Cr}53) + 0.027 \sigma(\text{Cr}52)$ , Arrows indicate  $^{52}\text{Cr}$  resonances

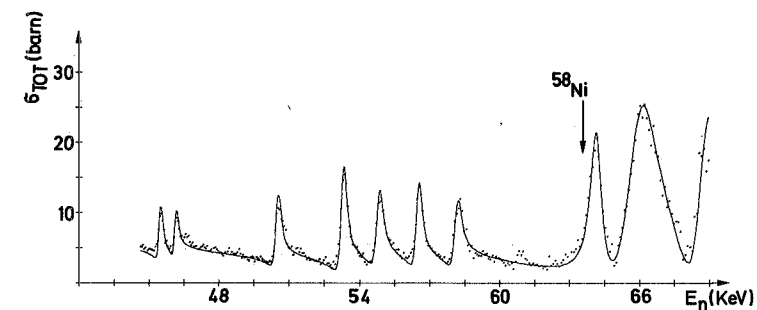
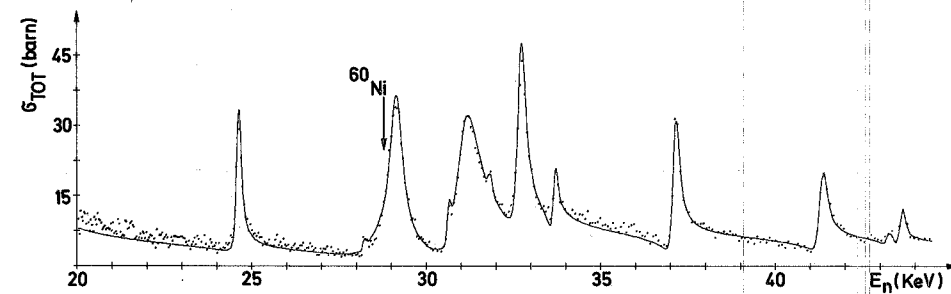
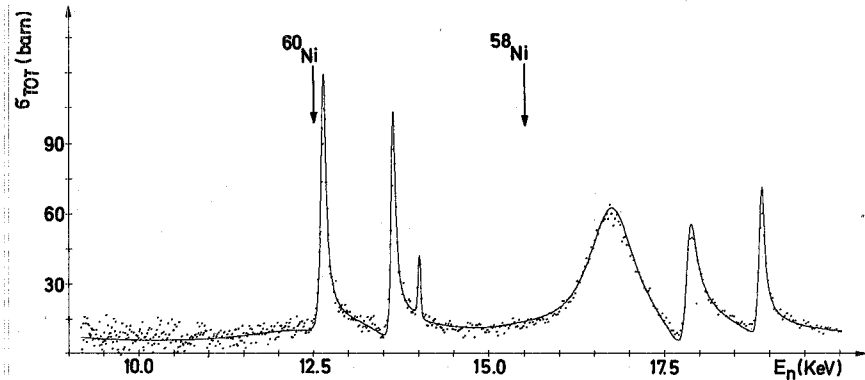
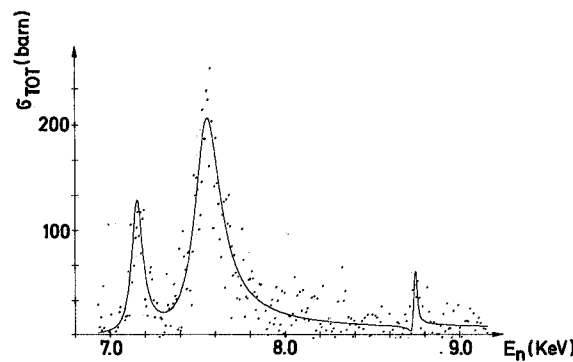


Fig. 5. Total neutron cross section curve for  $^{61}\text{Ni}$   
0.9178  $\sigma(\text{Ni } 61)$  + 0.052  $\sigma(\text{Ni } 60)$  + 0.021  $\sigma(\text{Ni } 58)$

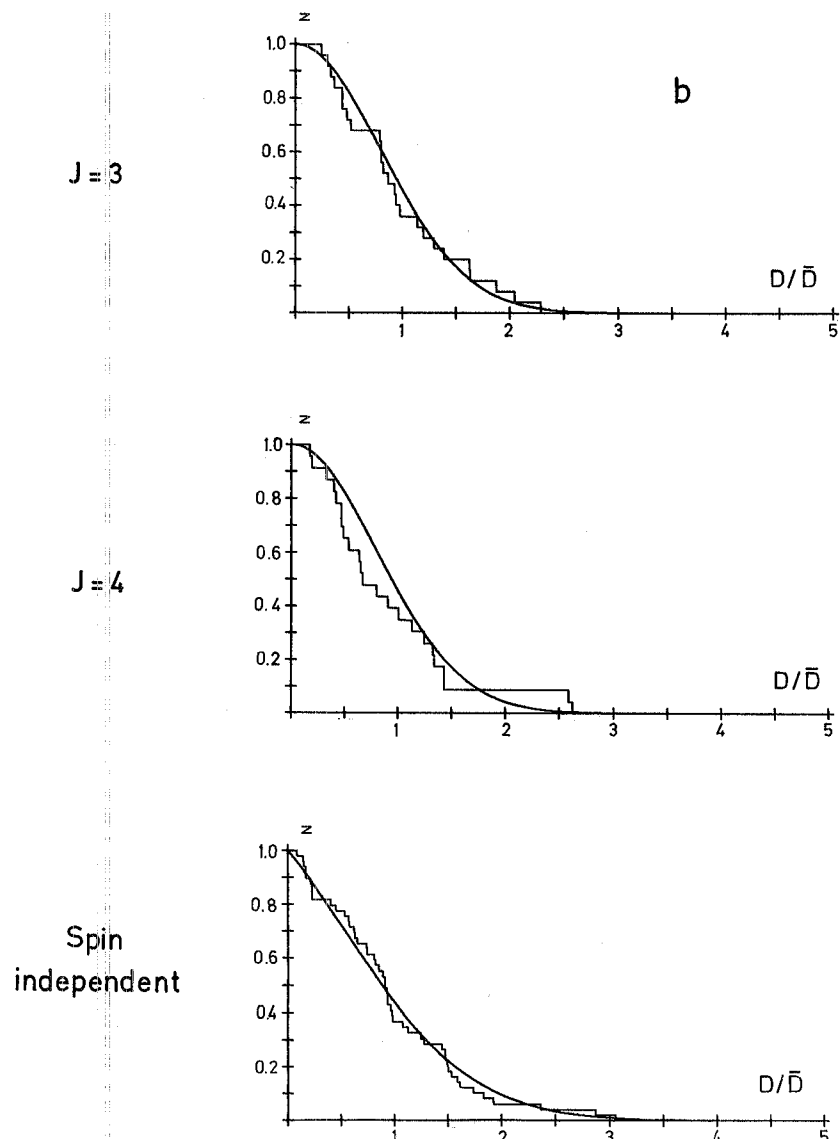
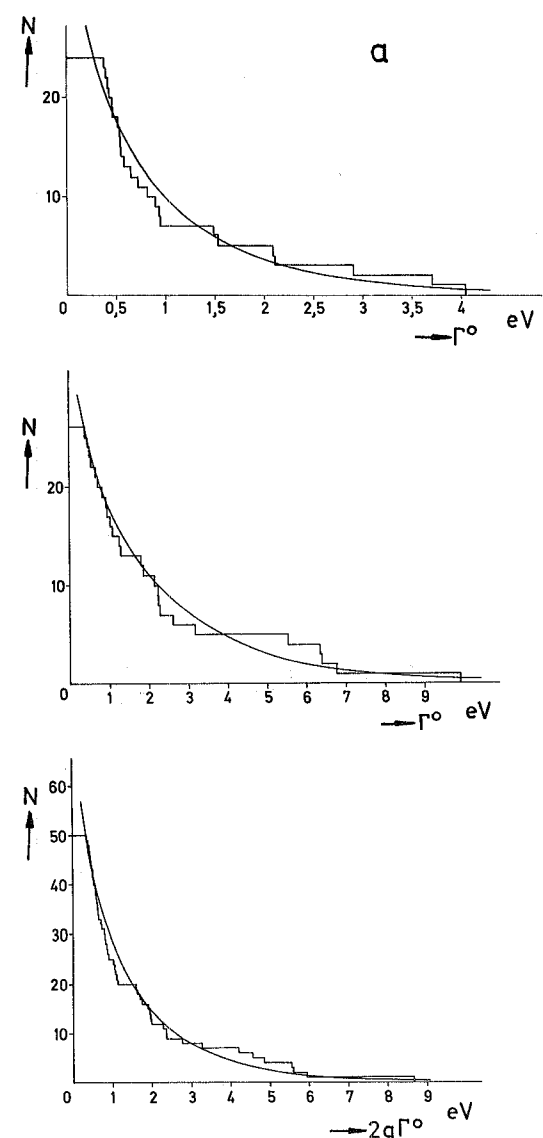


Fig. 6. Distribution of widths (a) and spacings (b) for  $^{45}\text{Sc} + \text{n}$